

## Article

# Magnetically Agitated Nanoparticle-Based Batch Reactors for Biocatalysis with Immobilized Aspartate Ammonia-Lyase

Ali Obaid Imarah <sup>1,2</sup>, Pál Csuka <sup>1</sup>, Naran Bataa <sup>1</sup>, Balázs Decsi <sup>1</sup>, Evelin Sánta-Bell <sup>1</sup>, Zsófia Molnár <sup>1,3,4</sup>,  
Diána Balogh-Weiser <sup>1,5,6</sup>  and László Poppe <sup>1,6,7,\*</sup> 

<sup>1</sup> Department of Organic Chemistry and Technology, Budapest University of Technology and Economics, Műegyetem rkp. 3, H-1111 Budapest, Hungary; aal-alwani@edu.bme.hu (A.O.I.); csuka.pal@vbk.bme.hu (P.C.); nbataa221@edu.bme.hu (N.B.); balazsdecsi@edu.bme.hu (B.D.); santa-bell.evelin@vbk.bme.hu (E.S.-B.); molnar.zsofia@vbk.bme.hu (Z.M.); balogh.weiser.diana@vbk.bme.hu (D.B.-W.)

<sup>2</sup> Chemical Engineering Department, College of Engineering, University of Babylon, Hilla Babylon 5100, Iraq

<sup>3</sup> Fermentia Microbiological Ltd., Berliini út 47-49, H-1045 Budapest, Hungary

<sup>4</sup> Institute of Enzymology, Research Center for Natural Sciences, Hungarian Academy of Science, Magyar tudósok körútja 2, H-1117 Budapest, Hungary

<sup>5</sup> Department of Physical Chemistry and Materials Science, Budapest University of Technology and Economics, Műegyetem rkp. 3, H-1111 Budapest, Hungary

<sup>6</sup> SynBiocat Ltd., Szilasliget u 3, H-1172 Budapest, Hungary

<sup>7</sup> Biocatalysis and Biotransformation Research Center, Faculty of Chemistry and Chemical Engineering, Babeş-Bolyai University of Cluj-Napoca, Arany János Str. 11, RO-400028 Cluj-Napoca, Romania

\* Correspondence: poppe.laszlo@vbk.bme.hu; Tel.: +36-1-463-3299



**Citation:** Imarah, A.O.; Csuka, P.; Bataa, N.; Decsi, B.; Sánta-Bell, E.; Molnár, Z.; Balogh-Weiser, D.; Poppe, L. Magnetically Agitated Nanoparticle-Based Batch Reactors for Biocatalysis with Immobilized Aspartate Ammonia-Lyase. *Catalysts* **2021**, *11*, 483. <https://doi.org/10.3390/catal11040483>

Academic Editor: Ulf Hanefeld

Received: 19 March 2021

Accepted: 7 April 2021

Published: 9 April 2021

**Publisher's Note:** MDPI stays neutral with regard to jurisdictional claims in published maps and institutional affiliations.



**Copyright:** © 2021 by the authors. Licensee MDPI, Basel, Switzerland. This article is an open access article distributed under the terms and conditions of the Creative Commons Attribution (CC BY) license (<https://creativecommons.org/licenses/by/4.0/>).

**Abstract:** In this study, we investigated the influence of different modes of magnetic mixing on effective enzyme activity of aspartate ammonia-lyase from *Pseudomonas fluorescens* immobilized onto epoxy-functionalized magnetic nanoparticles by covalent binding (AAL-MNP). The effective specific enzyme activity of AAL-MNPs in traditional shake vial method was compared to the specific activity of the MNP-based biocatalyst in two devices designed for magnetic agitation. The first device agitated the AAL-MNPs by moving two permanent magnets at two opposite sides of a vial in  $x$ -axis direction (being perpendicular to the  $y$ -axis of the vial); the second device unsettled the MNP biocatalyst by rotating the two permanent magnets around the  $y$ -axis of the vial. In a traditional shake vial, the substrate and biocatalyst move in the same direction with the same pattern. In magnetic agitation modes, the MNPs responded differently to the external magnetic field of two permanent magnets. In the axial agitation mode, MNPs formed a moving cloud inside the vial, whereas in the rotating agitation mode, they formed a ring. Especially, the rotating agitation of the MNPs generated small fluid flow inside the vial enabling the mixing of the reaction mixture, leading to enhanced effective activity of AAL-MNPs compared to shake vial agitation.

**Keywords:** magnetic agitation; magnetic nanoparticles; reactor design; aspartate ammonia-lyase; enzyme immobilization

## 1. Introduction

Sustainable and environmentally conscious development requires the advancement and application of economical, efficient, and green processes to meet the needs of different industries and users. Among the solutions suitable for the production of various materials to satisfy these needs, efficient catalytic technologies come to the fore, within which the ever-evolving biocatalytic processes play an important role [1,2]. In addition to the search for and development of newer and more efficient enzymes, the efficient development of biocatalysis requires that the mode of application of the biocatalysts should also be significantly improved [1,2].

### 1.1. Bioreactor Designs Using Agitated Magnetic Particles

A bioreactor is the heart of any biochemical process in which a wide variety of useful biological products are processed using enzymes, microbial, or plant cell systems [3].

Magnetic mixing reactor (MMR) using paramagnetic internal elements within a reactor agitated by an external magnetic field is a well-known way of mixing. A unique way of implementation is when the internal paramagnetic element is powder-like. The basic principle of magnetic mixing was first described by the patents of Hershler in 1965 [4,5]. Since then, various reports have been published on the application of a magnetic mixing reactor and many reactor designs have been developed mostly for biocatalytic processes [6]. In a flow-through magnetic fluidized bed reactor system (MFBR), superparamagnetic nanoparticles covered by immobilized lipase as a biocatalyst were agitated by alternating magnetic field generated by electromagnets of variable strengths and frequencies [7]. In a magnetically stirred reactor (MSR), a reactor operated in batch mode was fixed in the coil rack such that the reactor volume was completely immersed into the magnetic field [8]. A magnetically retained enzyme reactor (MRER) with immobilized cholesterol esterase and cholesterol oxidase on magnetic nanoparticles (MNPs) anchored in the reaction/detection zone of a flow injection (FI) system has been used for the determination of total cholesterol in serum samples [9]. Y-intersection devices enabling fix-and-release of magnetic beads by a permanent magnet as a microfluidic platform were applied for the isolation of T cells from blood samples [10]. A magnetic responsive system anchoring pectinase-coated MNPs by a static permanent magnet over a filter membrane was applied as a biocatalytic membrane reactor (BMR) for continuous flow operation [11]. A magnetically stabilized fluidized bed reactor (MSFBR) using magnetic solenoid around a tube reactor filled with lipase-coated MNPs was applied for biolubricant production from castor oil [12]. A rotating magnetic field (RMF) generated by two permanent magnet bars rotating besides a micro-reactor (2 cm i.d. and 20 cm length, filled with co-crosslinked MNPs with a lipase as biocatalyst) was used for synthesis of butyl oleate [13]. These examples indicate that bioreactors based on enzyme-coated, magnetically agitated nanoparticles provide an appealing way of performing biotransformations. Since strong permanent neodymium magnets—developed in 1984 [14,15]—are available commercially in different sizes and shapes, use of them seems advantageous.

### 1.2. Magnetic Nanoparticles (MNPs) as Carrier for Enzyme Immobilization

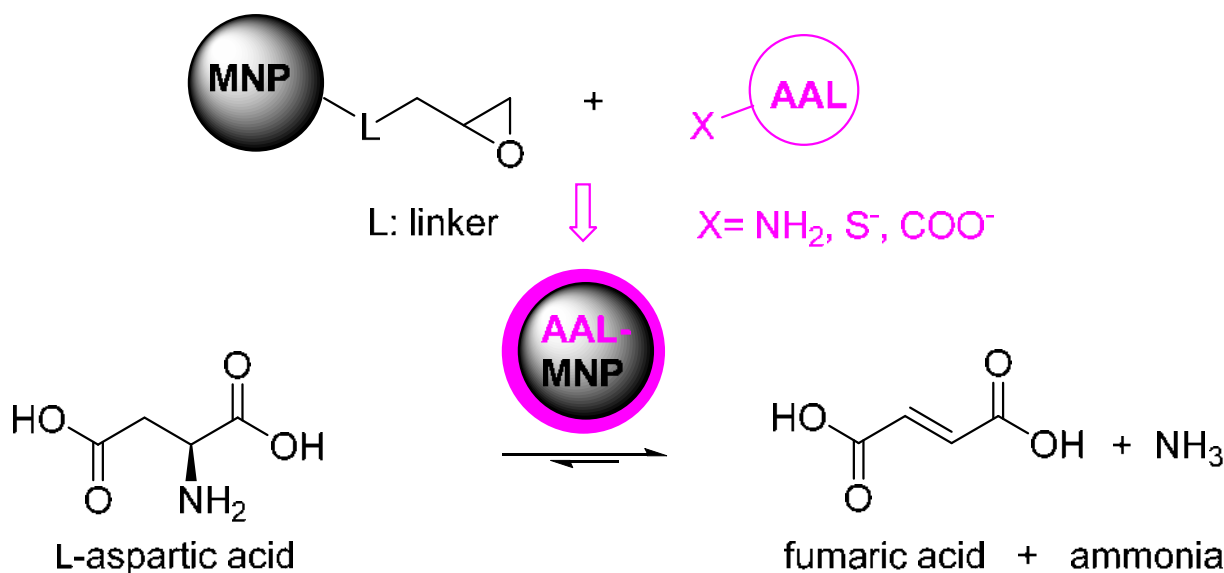
Magnetic nanoparticles are most often particles of iron oxide with various shapes and a diameter of about 1 to ~500 nm. The two main forms of superparamagnetic iron oxide are magnetite ( $\text{Fe}_3\text{O}_4$ ) and its oxidized form, maghemite ( $\gamma\text{-Fe}_2\text{O}_3$ ). Due to their special properties, they have aroused widespread interest and have already been applied in various ways in many fields [16,17]. The magnetic nanoparticles (MNPs) could be coated by enzymes and used as biocatalyst MNPs in a chip-sized flow-through reactor with cells containing magnetically anchored MNP biocatalysts in bioreaction screening applications [18,19]. The performance of the MNP-based magnetic systems depend on behavior of the MNPs under influence of the magnetic field, which is related to the magnetic force, Stokes drag, and diffusive motions [20]. With an emphasis on enzyme immobilization, the magnetic properties of nanoparticles and their low toxicity have attracted attention to their use in various fields of biotechnology. Some of the superior features of these materials are the high surface area, low mass transfer resistance, and ease of enzyme isolation from the reaction mixture relative to other supports used for enzyme immobilization [21,22]. Mass transfer resistance at the boundary surface of a particle plays a crucial role among others in heterogeneous catalysis as well as in sorption from strongly diluted solutions, as it may often limit the total reaction rate [8]. It is therefore of particular interest to accelerate mass transfer in such systems. Solid MNP-based carriers have large surface area, and the smaller the diameter, the higher the surface area vs. volume ratio. Due to the easy magnetic recovery of MNPs, many more applications are being investigated. For example, immobilization of a homotetrameric phenylalanine ammonia-lyase (PAL) on properly

activated magnetic nanoparticles has been developed [18,19]. The PAL-MNP preparations proved to be highly useful biocatalysts in chip-sized reactors comprising cells filled with the biocatalyst.

### 1.3. Aspartate Ammonia-Lyases

Enzymes can greatly increase the rate of some chemical reactions and thus can act as a biocatalyst. Aspartate ammonia-lyases (AAL)—also referred to as aspartases [23]—are microbial enzymes that play a key role in nitrogen metabolism by catalyzing the elimination of ammonia from L-aspartate to yield fumarate [8,23–25]. AALs have been characterized from Gram-negative and Gram-positive bacteria [25]. Because the reaction catalyzed by aspartate ammonia-lyases is reversible, AALs could be used to produce enantiopure L-aspartic acid (being an important starting compound for the synthesis of food additives and artificial sweeteners) on a large scale [26,27]. Although early studies showed strict substrate tolerance of AALs accepting only L-aspartic acid as substrate in deamination reaction [23–25], later works enabled the synthesis of *N*-substituted aspartic acids with AAL-catalysis [28]. After computational redesign, the engineered bacterial AAL could even catalyze asymmetric addition of ammonia to substituted acrylates, affording enantiopure aliphatic, polar, and aromatic  $\beta$ -amino acids that are valuable building blocks for the synthesis of pharmaceuticals and bioactive compounds [29].

Since the major aim of this study was to investigate the magnetic agitation of enzymes immobilized on magnetic nanoparticles as a biocatalyst in various modes, an enzyme of high biocatalytic efficiency but sensitivity for consequences of shearing forces was required. The potential of AALs as promising biocatalysts characterized with high catalytic efficiency and homotetrameric structure [24] rendered AAL as the enzyme of choice for our present study. Since magnetic nanoparticles were successfully applied for the structurally similar PAL [18,19], the selected aspartate ammonia-lyase from *Pseudomonas fluorescens* [30] was immobilized on similar epoxy-functionalized MNPs for the studies with magnetically agitated MNP biocatalyst. The resulted aspartate ammonia-lyase biocatalyst (AAL-MNP) has been characterized by its natural reaction converting L-aspartate to fumarate (Scheme 1).



**Scheme 1.** Immobilization of aspartate ammonia-lyase (AAL) on a magnetic nanoparticle (MNP) and conversion of L-aspartate to fumarate with the immobilized biocatalyst (AAL-MNP).

## 2. Results and Discussion

As we found no batch reactor implementation of magnetically agitated MNPs, our goal in this study was to design devices applicable for magnetic mixing of MNPs for

batch biotransformations. Although there are regular shakers, in a shake vial (SH), the biocatalyst fixed to the MNPs move along with the liquid phase of the reaction—containing the reaction components—in the same direction (Figure 1). Thus, the relative movements of the MNP biocatalysts and the reaction medium is small. Moreover, in a real shake vial implementation without magnetic agitation, a significant portion of the MNP-based biocatalyst sticks to the wall by adsorption. Obviously, this portion of the biocatalyst plays hardly any role in the reaction.

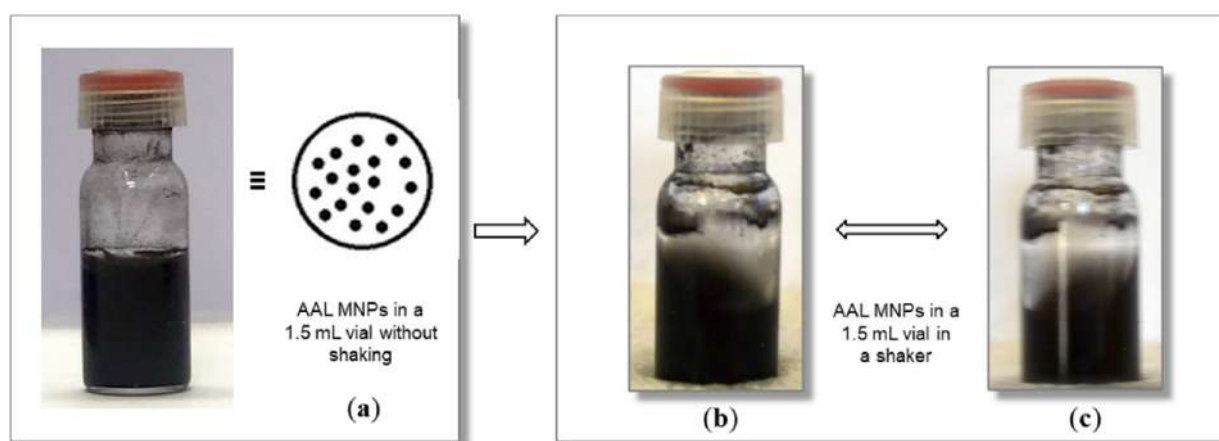


**Figure 1.** The aspartate ammonia-lyase biocatalyst immobilized on magnetic nanoparticles (AAL-MNPs) (a) as a suspension in a non-agitated vial and (b,c) in a reaction performed in a shake vial (SH). Pictures (b,c) show two opposite-position states of the reaction vial in a real orbital shaker (note the significant portion of AAL-MNPs stuck on the wall).

In a real reaction implementation using heterogenized enzyme as a biocatalyst, the kinetics can be quite complex, and the effective rate (thereby the effective specific activity) depends not only on the inherent kinetic behavior of the enzyme but is usually influenced by the various parameters of the process [31].

In this study, our major aim was to compare the influence of the modes of agitation on the effective catalytic activity of a magnetic nanoparticle-based biocatalyst. The enzyme for this study was the aspartate ammonia-lyase from *Pseudomonas fluorescens* immobilized onto magnetic nanoparticles (AAL-MNPs). The magnetically agitated reaction modes were compared to shake vial suspension of the AAL-MNPs in a regular orbital shaker with 650 rpm at room temperature (20 °C) as reference.

Transport phenomena occurring in micro devices can be more easily subjected to theoretical study and accurate control because of the well-defined geometry, short transport distances, and fast transients than those in larger-scale systems [32]. Therefore, we designed our study in small scale (1 mL, with 5 mg of AAL-MNPs), in tubular parts of small vials (ID = 9.5 mm). For agitation of the AAL-MNPs in a vial by two permanent magnets, two basic modes of agitation were designed. In the first case—referred as axial agitation mode (XM)—the two permanent magnets in fixed distances were moving along the  $x$ -axis, being perpendicular to the  $y$ -axis of the AAL-MNP-containing vial. In the second case—referred to as rotating agitation mode (RM)—the two permanent magnets in fixed distances were rotated around the  $y$ -axis of the AAL-MNP-containing vial.

Depending on their possible relative arrangements (attraction ( $_{att}$ ) and repulsion ( $_{rep}$ )), the two permanent magnets generated basically different magnetic fields (Figure 2). Therefore, two implementations should be considered for each agitation modes ( $XM_{att}$  and  $XM_{rep}$  for the axial agitation mode, and  $RM_{att}$  and  $RM_{rep}$  for the rotating agitation mode).

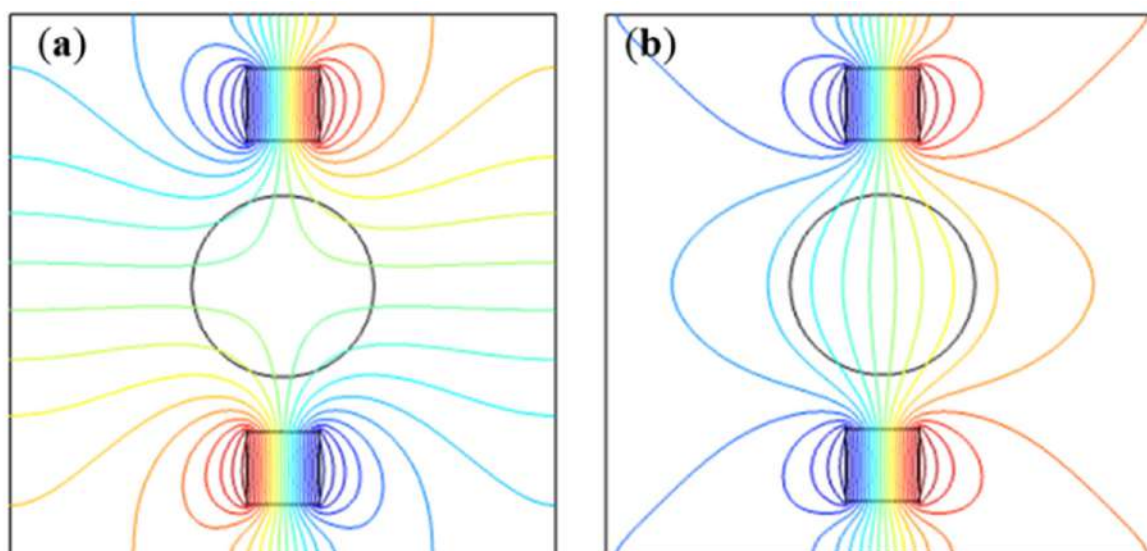


**Figure 2.** Qualitative representation of the fields generated by two permanent magnets (a) in attraction arrangement ( $att$ ) and (b) in repulsion arrangement ( $rep$ ).

### 2.1. Mixing the AAL-MNPs in Axial Agitation Mode Devices (XM)

In the first device for axial agitation of the AAL-MNPs along the  $x$ -axis direction, two permanent neodymium magnets (N48, rings of  $10 \times 5 \times 5$  mm) were fixed at opposite sides of the centrally positioned sample vial (1.5 mL) containing the reaction mixture (Figure 3).

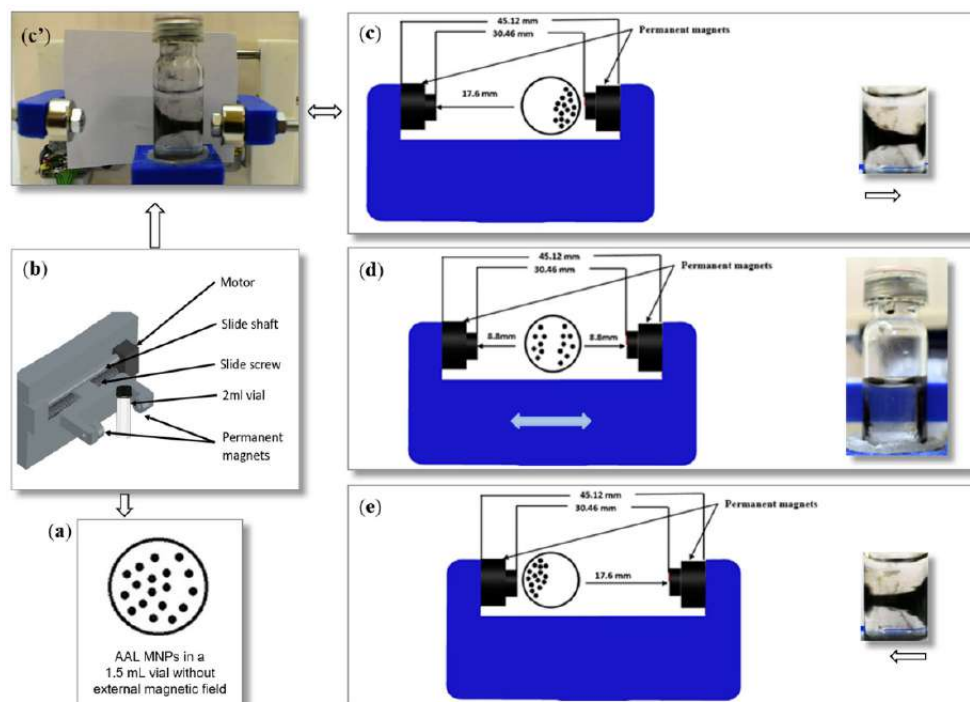


**Figure 3.** A device for axial magnetic agitation of aspartate ammonia-lyase immobilized on magnetic nanoparticles (AAL-MNPs). The vial containing AAL-MNPs (a) was placed in a device (b,c) capable of moving two permanent magnets in fixed distances along the  $x$ -axis, being perpendicular to the  $y$ -axis of the AAL-MNP-containing vial. Images (c,e) depict the behavior of the MNP-cloud at the two end positions of the movement along the  $x$ -axis with the magnets positioned in attraction mode ( $XM_{att}$ ); (d) shows the mid position (note that negligible portion of AAL-MNPs stuck on the wall of the vial due to the magnetic agitation). The movement frequency is characterized by the mpm (movement per minute) value.

The results with axial agitation mode using the two possible magnet configurations ( $XM_{att}$  and  $XM_{rep}$ ; generating two different magnetic fields) were compared to AAL-MNPs containing vials in orbital lab shaker (SH; operated at 650 rpm and 20 °C) as reference (Figure 4).

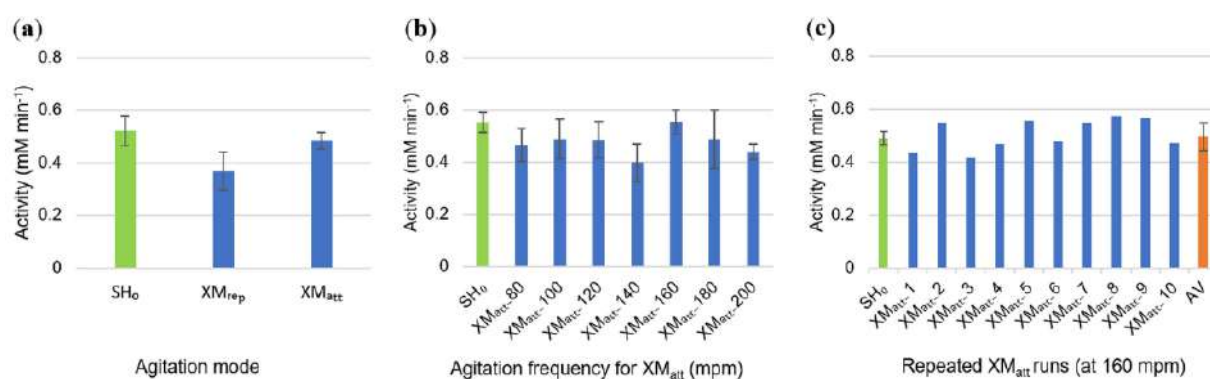


**Figure 4.** Investigation of the axial agitation mode with AAL-MNPs. (a) Dependence of the effective enzyme activity on permanent magnet configuration ( $XM_{att}$ : attraction configuration,  $XM_{rep}$ : repulsion configuration; at 120 MPM) compared to shaking mode with fresh AAL-MNPs ( $SH_0$ ). (b) Dependence of the effective enzyme activity on the frequency of movement along the  $x$ -axis ((using the  $XM_{att}$  mode, in movement per minute (mpm), within the 80–200 mpm range). (c) Investigation of operational stability (repeatability) of the AAL-MNP reaction by  $XM_{rep}$  mode at 160 mpm (the biocatalyst was used 10 times after recovery by magnetic decantation). The results and their average (AV) are compared to shaking mode with fresh AAL-MNPs ( $SH_0$ ).

First, the two permanent magnet configurations were compared in the axial agitation mode ( $XM_{att}$  and  $XM_{rep}$ , at 120 mpm) for the AAL-MNP-catalyzed ammonia elimination reaction from L-aspartate to fumarate (Figure 4a). Although the effective activity was not higher in any of the axial agitation modes at 120 mpm than that of the shake vial mode ( $SH_0$ ), the result with attraction configuration of permanent magnets in the axial agitation mode ( $XM_{att}$ ) was significantly better than with the repulsion configuration ( $XM_{rep}$ ). In attraction configuration of the axial agitation mode ( $XM_{att}$ ), a cloud of MNPs moved from one side of the vial to the other (Figure 3c–e), resulting in a small movement of fluid around the cloud, effecting all the liquid inside the vial. Apparently, in this agitation mode, the mechanical drag force from the action of the magnetic field on the MNPs was in good balance with the shearing force coming from the viscosity of the liquid. Contrarily, when repulsion configuration of the axial agitation mode ( $XM_{rep}$ ) was applied, the MNPs also formed a cloud but moved in half elapse in the bottom of the vial, which is not sufficient for good mixing inside the vial. It is notable that only negligible amounts of MNPs stuck on the wall of the vial (Figure 3), in contrast to the shake vial experiments (Figure 1).

Due to the significantly better activity achievable with the attraction configuration of the axial agitation mode than with the repulsion configuration, the optimal frequency of movement was investigated only with the attraction setup ( $XM_{att}$ ; Figure 4b). Although an optimum of the effective activity of the reaction was observed at 160 mpm frequency ( $U_{160\text{ mpm}} = 0.55\text{ mM min}^{-1}$ ), this effective activity did not differ significantly from that of the reference reaction in the shake vial ( $SH_0$ ,  $U_0 = 0.55\text{ mM min}^{-1}$ ).

Finally, a test was performed using the attraction configuration of the axial agitation mode ( $XM_{att}$ ) at the optimal 160 mpm frequency to investigate how the reaction conditions and mode of agitation affect the enzyme activity of AAL-MNPs (Figure 4c). Thus, the test reaction was repeated 10 times at the optimum frequency of agitation using the same AAL-MNP biocatalyst for each repetition, indicating that the shearing forces were not detrimental for the biocatalytic activity under these conditions within the investigated timeframe. In this respect, the AAL-MNPs in  $XM_{att}$  mode were similarly stable over 10 cycles of repeated reactions as in  $SH_0$  mode (data not shown).

## 2.2. Mixing the AAL-MNPs in Rotating Agitation Mode Devices (XM)

The other device for rotating agitation of the AAL-MNPs around the  $y$ -axis of the central vial also applied two permanent neodymium magnets (N48, rings of  $10 \times 5 \times 5$  mm) fixed at opposite sides of the sample vial (1.5 mL) containing the reaction mixture (Figure 5). Like for the previous set of investigations, the results with rotation agitation mode using the two possible magnet configurations ( $RM_{att}$  and  $RM_{rep}$ ; generating two different magnetic fields) were compared to the reaction in shake vials (SH; Figure 6).

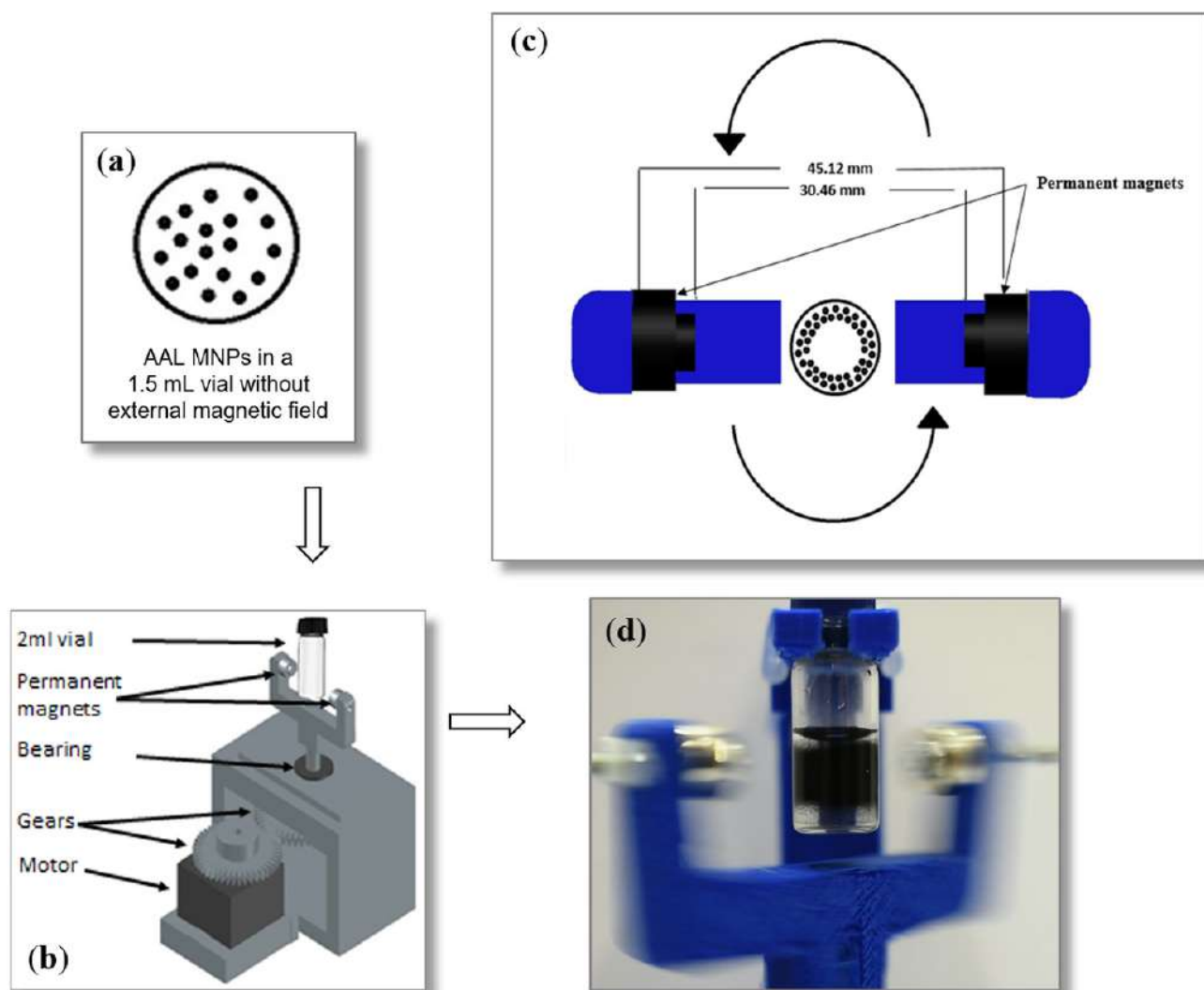


**Figure 5.** A device for rotating magnetic agitation of aspartate ammonia-lyase immobilized on magnetic nanoparticles (AAL-MNPs). The vial containing AAL-MNPs (a) was placed in a device (b) capable of rotating two permanent magnets in fixed distances around the  $y$ -axis of the centrally positioned AAL-MNP-containing vial (c,d). The external magnetic field generated by the two rotating permanent magnets in attraction configuration ( $RM_{att}$ ) resulted in a ring-shaped MNP cloud (c,d). The movement frequency is characterized by the rpm (rotation per minute) value.

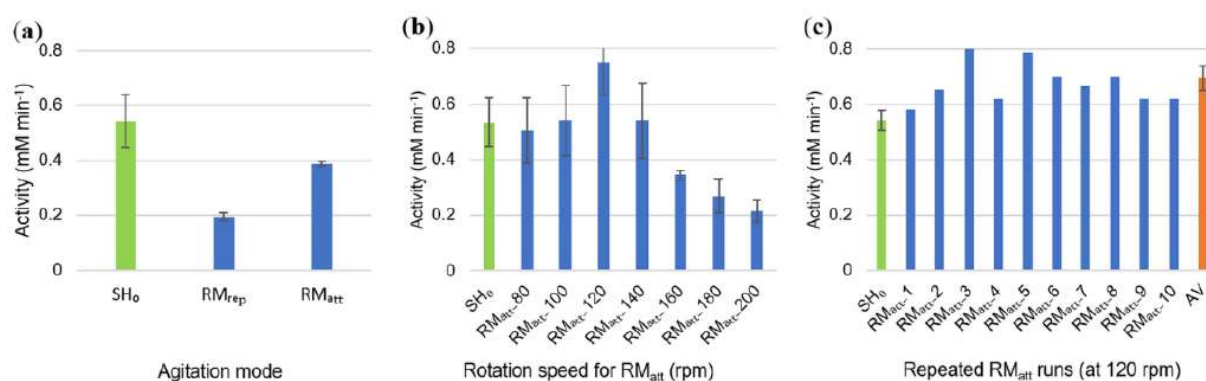


**Figure 6.** Investigation of the rotating agitation mode with AAL-MNPs. (a) Dependence of the effective enzyme activity on permanent magnet configuration (RM<sub>att</sub>: attraction configuration, RM<sub>rep</sub>: repulsion configuration; at 150 rpm) compared to shaking mode with fresh AAL-MNPs (SH<sub>0</sub>). (b) Dependence of the effective enzyme activity on the frequency of rotation around the  $y$ -axis of the vial (using the RM<sub>att</sub> mode, in rotation per minute (rpm), within the 80–200 rpm range). (c) Investigation of operational stability (repeatability) of the AAL-MNP reaction by RM<sub>rep</sub> mode at 120 rpm (the biocatalyst was used 10 times after recovery by magnetic decantation). The results and their average (AV) are compared to shaking mode with fresh AAL-MNPs (SH<sub>0</sub>).

As for the previous set of experiments, first the two permanent magnet configurations in the rotating agitation mode (RM<sub>att</sub> and RM<sub>att</sub>, at 150 rpm) for the AAL-MNP catalyzed reaction were compared to the shake vial mode (SH<sub>0</sub>) (Figure 6a). At 150 rpm selected for the comparison, the effective activity was not higher in any of the rotating agitation modes than that of the shake vial mode (SH<sub>0</sub>). However, the result with attraction configuration of the rotating agitation mode (RM<sub>att</sub>) was significantly better than with the repulsion configuration (RM<sub>rep</sub>). The attraction configuration of rotating agitation mode (RM<sub>att</sub>) resulted in the formation of a ring-shaped cloud of MNPs moving around the  $y$ -axis of the vial (Figure 5c,d), which stirred the whole amount of fluid around the cloud inside the vial. As a result of magnetic dragging of the AAL-MNPs in the rotating agitation mode with attraction configuration (RM<sub>att</sub>), practically no biocatalyst stayed on the wall of the vial (Figure 5d), like in the axial agitation mode experiments with attraction configuration (Figure 3c–e). When the repulsion configuration was applied for the rotating agitation mode (RM<sub>rep</sub>), all the AAL-MNPs were moving around the bottom of vial and the mixing could not affect the full amount of reaction medium.

Next, the optimal speed of rotation was investigated with the more efficient attraction configuration (RM<sub>att</sub>; Figure 6b). The effective activity of the MNP biocatalyst with RM<sub>att</sub> agitation at the optimal rotation speed (120 rpm:  $U_{120 \text{ rpm}} = 0.75 \text{ mM min}^{-1}$ ) was significantly higher than in shake vial mode (SH<sub>0</sub>:  $U_0 = 0.53 \text{ mM min}^{-1}$ ). Apparently, at the optimum speed of rotation (120 rpm), the drag force of the magnetic field and the centrifugal force of mechanical movement was at an optimal balance with the shear force, which came from the viscosity of liquid. This means a complex balance, including MNP movement relative to the bulk liquid and stirring the whole volume of liquid by all the MNPs in the cloud, resulting in enhancement of mass transport, not only in the close neighborhood of the AAL-MNPs, but in the whole volume of the reaction mixture.

The attraction configuration of the rotating agitation mode at the optimal rotation speed (RM<sub>att</sub>, 120 rpm) was also investigated for longer term stability of the AAL-MNPs (Figure 6c). The test reaction in the RM<sub>att</sub> mode was repeated 10 times with the same AAL-MNP biocatalyst in each cycle showing good stability of the biocatalytic activity under the rotating agitation conditions within the timeframe of recycling study. The recycling study also confirmed the significant improvement of the effective activity by this agitation mode (the average activity of the 10 repeated reactions ( $U_{\text{av } 120 \text{ rpm}} = 0.70 \text{ mM min}^{-1}$ ) exceeded by 30% of the effective activity of AAL-MNPs in the shake vial (SH<sub>0</sub>:  $U_0 = 0.54 \text{ mM min}^{-1}$ )).

### 2.3. Effective Kinetic Parameters of AAL in Rotating Agitation Mode Device

Even in the simplest case with a single enzyme following Michaelis–Menten kinetics attached to a surface, the kinetics can be quite complex depending on microenvironmental effects, diffusional resistances, and kinetic complications occurring simultaneously [31,33,34]. Internal diffusional limitation plays significant roles mostly for enzymes embedded in a porous matrix but may be negligible in the case of an enzyme attached to the surface of MNPs. However, strict treatment of the effect of external diffusion on heterogeneous enzyme kinetics requires accurate knowledge of the hydrodynamic conditions of the fluid and the integration of a differential equation corresponding to the exact boundary conditions expressing the retention of the substrate and the product. In fact, the effective rate of the reaction ( $V$ ) depends both on the mass transport coefficient for the substrate ( $h_s$ ) and the kinetic parameters of the reaction ( $V_{\max}$  and  $K_M$ ) and on the local substrate concentration ( $[S]$ ) [31]. The effective rate is usually more strongly influenced by the parameters of one process than by those of the other.

Thus, after finding the optimal rotation speed for  $RM_{\text{att}}$  agitation mode (120 rpm), the kinetic behavior of the AAL-MNPs biocatalyst was studied in the magnetically agitated reactor. The effective Michaelis–Menten constants ( $K_M$  and  $k_{\text{cat}}$ ;  $k_{\text{cat}} = V_{\max}/E_0$ ) for comparing the various reaction modes were determined based on the  $V = V_{\max} \times [S]/(K_M + [S])$  equation. The effective Michaelis–Menten constants of the aspartate ammonia-lyase from *P. fluorescens* R123 in the best agitation mode ( $RM_{\text{att}}$ , 120 rpm;  $K_M = 7.1$  mM and  $k_{\text{cat}} = 8.9$  s<sup>-1</sup>)—determined in this work—were compared to the kinetic behavior of the AAL in homogenous solution and the AAL-MNPs in the shake vial (Table 1, Figure S1, Table S1) [30].

**Table 1.** Effective kinetic parameters of aspartate ammonia-lyase in various reaction modes <sup>a</sup>.

Biocatalyst	Reactor Type	$K_M$ (mM)	$V_{\max}$ ( $\mu\text{M s}^{-1}$ )	$k_{\text{cat}}$ (s <sup>-1</sup> )	$k_{\text{cat}}/K_M$ (mM <sup>-1</sup> s <sup>-1</sup> )	Ref.
native AAL <sup>b</sup>	shake vial <sup>d</sup>	5.1	3.6	129.7	25.3	[30]
AAL-MNP <sup>c</sup>	shake vial <sup>d</sup>	18.4	11.2	20.1	1.1	[30]
AAL-MNP <sup>c</sup>	$RM_{\text{att}}$ reactor <sup>e</sup>	7.1	5.0	8.9	1.3	

<sup>a</sup> Reaction conditions: 50 mM Tris buffer, pH = 8.8; 30 °C, L-aspartate concentration: 0.01–60 mM; <sup>b</sup> AAL molar concentration (monomeric unit) for native AAL:  $E_0 = 0.028$   $\mu\text{M}$  (1.5  $\mu\text{g mL}^{-1}$ ); <sup>c</sup> AAL molar concentration (monomeric unit) for AAL-MNP reactions (1 mL reaction volume containing 5 mg mL<sup>-1</sup> AAL-MNPs with 6  $\mu\text{g mg}^{-1}$  AAL on the MNP):  $E_0 = 0.56$   $\mu\text{M}$  (30  $\mu\text{g mL}^{-1}$ ); <sup>d</sup> at 600 rpm; <sup>e</sup> at 120 rpm.

The decreased  $k_{\text{cat}}$  for the AAL-MNP reactions ( $k_{\text{cat}} = 20.1$  s<sup>-1</sup> for  $SH_0$  and  $k_{\text{cat}} = 8.9$  s<sup>-1</sup> for  $RM_{\text{att}}$ ) compared to the reaction with native AAL ( $k_{\text{cat}} = 129.7$  s<sup>-1</sup>) can be attributed mostly to diffusional effects (the shortest path from bulk to an enzyme is required for the homogenous enzyme solution) and less to conformational and spatial restrictions due to enzyme immobilization. Formation of the AAL-MNP-cloud and a catalyst-free region in the  $RM_{\text{att}}$  reaction elongate the average diffusional path from bulk to biocatalyst compared to the  $SH_0$  situation, thus resulting in smaller  $k_{\text{cat}}$ .

The similar  $K_M$  values in the reactions with native AAL and AAL-MNP in  $RM_{\text{att}}$  mode ( $K_M = 5.1$  mM for AAL and  $K_M = 7.1$  mM for  $RM_{\text{att}}$ ) indicate that no serious conformational and spatial restrictions happen by the immobilization on the MNPs. The virtually higher  $K_M$  value for the AAL-MNPs in  $SH_0$  mode ( $K_M = 18.4$  mM) as compared to the  $RM_{\text{att}}$  mode ( $K_M = 7.1$  mM) could be due to the slower relative movement of the liquid to AAL-MNPs in  $SH_0$  mode.

The higher enzyme efficiency characterized by the  $k_{\text{cat}}/K_M$  value for the native AAL ( $k_{\text{cat}}/K_M = 25.3$  mM<sup>-1</sup> s<sup>-1</sup>) could be rationalized less by the effect of enzyme conformational changes and more by diffusional limitations. In line with the activity measurements, among the AAL-MNP-catalyzed reaction modes, the AAL-MNPs were more efficient in the optimal  $RM_{\text{att}}$  mode ( $k_{\text{cat}}/K_M = 1.3$  mM<sup>-1</sup> s<sup>-1</sup>) as in the  $SH_0$  reaction ( $k_{\text{cat}}/K_M = 1.1$  mM<sup>-1</sup> s<sup>-1</sup>).

#### 2.4. Modulation of Viscosity on the AAL-MNP-Catalysis in Various Reaction Modes by Glycerol

Because glycerol can strongly modulate the viscosity of the reaction medium without altering the enzyme properties (glycerol is a known protective agent for storage of enzymes), we studied the magnetically agitated AAL-MNP biocatalysts in reactions containing various amounts of glycerol.

In this series of experiments, both magnetic agitation modes were investigated using the best configurations at optimum speed ( $XM_{att}$  at 160 mpm; and  $RM_{att}$  at 120 rpm) in media without and with 5, 10, and 15 v/v% added glycerol (Figure 7).

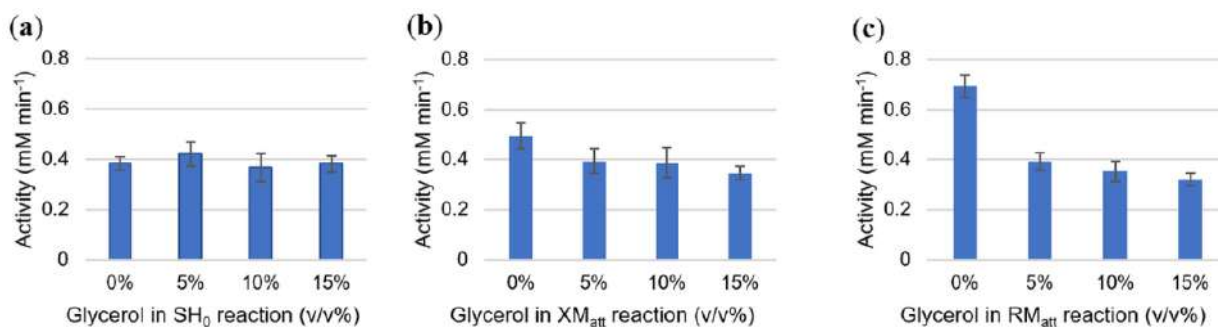


**Figure 7.** Comparison of the effective activity of AAL-MNPs in various agitation modes at different viscosities. The effective activity values of AAL-MNPs are shown in (a) the shake vial mode ( $SH_0$  at 650 rpm), in (b) the axial agitation mode ( $XM_{att}$  at 160 mpm), and in (c) the rotating agitation mode ( $RM_{att}$  at 120 rpm) at various viscosities of the reaction media (altered by adding 5%, 10%, and 15% glycerol to the reaction mixture).

The results indicated that rotation agitation mode ( $RM_{att}$  at 120 rpm) was the most efficient among the agitation modes at their optimal agitation speed (Figure 7c). It was also apparent that the effect of the increasing viscosity was less pronounced for the shake vial and axial agitation modes (Figure 7a:  $SH_0$  at 650 rpm; and Figure 7b:  $XM_{att}$  at 160 mpm) than for the rotation agitation mode (Figure 7c:  $RM_{att}$  at 120 rpm). Consequently, the diffusional limitations play more important roles in affecting the effective reaction rate of the AAL-MNP biocatalyst in  $RM_{att}$  mode. These results are also in line with the assumptions for rationalizing the effective kinetic constants for the two magnetic agitation modes.

### 3. Materials and Methods

**Materials:** Iron(III) chloride hexahydrate, sodium acetate trihydrate, tetraethoxysilane (TEOS), polyethylene glycols PEG 400, and PEG 4000, aminopropyltrimethoxysilane (APTMS), glycidol, glycerol diglycidyl ether (GDE), tris-(hydroxymethyl)amino-methane (Tris), L-aspartic acid, and fumaric acid were purchased from Merck KGaA (Darmstadt, Germany) or Alfa Aesar Europe (Karlsruhe, Germany).

**Solvents:** ethylene glycol, 2-propanol, ethanol, hexane were purchased from Merck Ltd. (Darmstadt, Germany). Patosolv® (a mixture of 10–15% 2-propanol and 85–90% ethanol) was a product of Molar Chemicals Ltd. (Budapest, Hungary).

#### 3.1. Preparation of Epoxy-Activated MNP Carrier

The preparation steps of the MNP-based enzyme carrier (MNP formation, silica shell preparation for MNPs, amine functionalization of silica-coated MNPs, and epoxy activation of the amine-functionalized MNPs) are described in the Supplementary Information Section S1.1.

#### 3.2. Immobilization of Aspartate Ammonia-Lyase on Epoxy-Activated MNPs

The enzyme immobilization of aspartase (AAL) onto epoxy-activated MNPs is described in the Supplementary Information Section S1.2.

### 3.3. Biocatalyst Activity Tests

The biocatalyst activity tests were performed in clean screw-capped vials (1.5 mL, 8–425 Vial Small Opening V813/V817, Aijiren Technology Inc., Quzhou, Zhejiang, China) using AAL-MNPs (5 mg) as a biocatalyst in the reaction mixture containing L-aspartic acid (20 mM) in Tris buffer (1 mL, 50 mM, pH = 8.8). All other reaction parameters are indicated as required. For sampling from reactions using different modes of agitation (orbital shaker, SH; two kinds of axial magnetic agitation modes,  $XM_{att}$  and  $XM_{rep}$ ; and two kinds of rotating magnetic agitation modes,  $RM_{att}$  and  $RM_{rep}$ ), samples (10  $\mu$ L) were taken from the reaction mixtures intermittently stopped at 2.5 min, 5 min, and 7.5 min.

For repeated activity tests, the reaction mixture was decanted from the AAL-MNP biocatalyst anchored by a strong neodymium permanent magnet and washed with Tris buffer (1 mL, 50 mM, pH = 8.8) for 2.5 min in the shaker. After decanting the washing solution, the AAL-MNP biocatalyst was filled up with a fresh reaction mixture containing L-aspartic acid (20 mM) in Tris buffer (50 mM, pH = 8.8). The activity tests were performed in triplicate.

The formation rate of the product fumarate was determined at  $\lambda = 210$  nm ( $\epsilon_{210} = 1.248$  mM<sup>-1</sup> mm<sup>-1</sup>) from an aliquot of the samples (3  $\mu$ L) with NanoDrop 2000 spectrophotometer (Thermo Fischer, Waltham, MA, USA). The product formation rate,  $v$  (given in mM min<sup>-1</sup>), was determined with linear regression and validated with the R<sup>2</sup> values.

### 3.4. Reactor Design and Assembly

The axial-movement agitation system and the rotation movement agitation system were designed by AutoCAD (2020 student version) program and printed by a Rankfor100 3D printer (CEI Conrad Electronic International, Ltd., New Territories, Hong Kong). The permanent magnets for this study were 10 × 5 × 5 mm N48 neodymium ring magnets ( $Br = 1.38$ – $1.42$  T/13.8–14.2 KGs,  $(B-H)_{max} = 46$ – $49$  MGOe/366–390 kJ/m<sup>3</sup>). The permanent magnets were agitated from a power supply (12 V, 5 A) by a NEMA17 motor (42 mm, 12 V, 1.5 A; Shenzhen Penghui Technology Co., Ltd., Shenzhen, China) controlled by an Arduino Uno microcontroller with L298 motor driver (Fut-Electronic Tech Co, Shenzhen, China) to control the movement of the two permanent magnet rings, facing each other in either attraction mode ( $_{att}$ ) or repulsion mode ( $_{rep}$ ) at fixed distance (30.5 mm; see Figures 3 and 5).

In the axial movement modes ( $XM_{att}$  and  $XM_{rep}$ ), the device depicted in Figure 3 moved the two permanent magnets positioned for attraction mode ( $_{att}$ ) or repulsion mode ( $_{rep}$ ) at fixed distance and the magnets were moved along an  $x$ -axis, being perpendicular to the axis of a screw-capped vial (1.5 mL,  $y$ -axis). The movement frequency is characterized by the mpm (movement per minute) value.

In the rotation movement modes ( $RM_{att}$  and  $RM_{rep}$ ), the device depicted in Figure 5 rotated the two permanent magnets positioned for attraction mode ( $_{att}$ ) or repulsion mode ( $_{rep}$ ) at fixed distance around the axis of a screw-capped vial (1.5 mL,  $y$ -axis). The rotation speed is characterized by the rpm (rotation per minute) value.

## 4. Conclusions

Our study focused on the influence of different modes of magnetic agitation on effective enzyme activity of aspartate ammonia-lyase from *Pseudomonas fluorescens* immobilized on magnetic nanoparticles (AAL-MNP) in biotransformations of L-aspartic acid performed in batch mode. The two magnetic agitation modes applied two permanent magnets fixed at two opposite sides of a vial containing the AAL-MNPs in the reaction medium in two configurations (attraction and repulsion arrangement). The first mode of agitation ( $XM$ ) moved the two permanent magnets axially (perpendicular to the axis of the vial), while the second mode of agitation ( $RM$ ) rotated the two permanent magnets around the axis of the vial. In both agitation modes, the attraction configurations proved to be more efficient and the speed of agitation had optima (160 mpm for  $XM_{att}$  and 120 rpm for  $RM_{att}$ ). While AAL-MNPs exhibited similar activity at their optimum in axial agitation mode ( $XM_{att}$ ) as in

traditional shake vial method ( $SH_0$ ), the effective specific activity of the MNP-based biocatalyst was ~30% higher at the optimum of rotation agitation mode ( $RM_{att}$ ). Apparently, the moving AAL-MNP cloud in the  $XM_{att}$  mode resulted in less efficient mixing inside the vial than the rotating ring-shaped cloud of the  $RM_{att}$  mode. Analysis of the effective enzyme kinetics constants and reaction viscosity modulation by added glycerol indicated that the effective rate of reaction is more diffusion-controlled in the  $RM_{att}$  mode than in the  $XM_{att}$  mode. Repeatability studies with both agitation modes revealed short-term resistance of the AAL-MNP biocatalyst against shearing forces and other reaction conditions. As a conclusion, magnetic agitation of enzymes immobilized on magnetic particles in various modes is a promising alternative of mixing of various bioreactors. The promising results of this study inspired us to implement similar modes of magnetic agitation in continuous flow devices in the future.

**Supplementary Materials:** The following are available online at <https://www.mdpi.com/article/10.3390/catal11040483/s1>, Figure S1: Michaelis–Menten enzyme kinetic of the immobilized aspartate ammonia-lyase (AAL-MNP) in rotation attraction agitation reactor mode ( $RM_{att}$ ) at 120 rpm; Table S1: Determination of the kinetic parameters of AAL-MNP biocatalyst with non-linear regression with Statistica software; Section S1.1: Preparation of epoxy-activated MNP carrier and Section S1.2: Immobilization of aspartate ammonia-lyase on epoxy-activated MNPs.

**Author Contributions:** Conceptualization, A.O.I. and L.P.; methodology, A.O.I., P.C., and L.P.; software, A.O.I.; investigation, A.O.I., P.C., N.B., B.D., E.S.-B., and Z.M.; resources, L.P.; writing—original draft preparation, A.O.I., P.C.; writing—review and editing, A.O.I., P.C., Z.M., and L.P.; supervision, L.P. and D.B.-W.; project administration, L.P. and D.B.-W.; funding acquisition, L.P. and D.B.-W. All authors have read and agreed to the published version of the manuscript.

**Funding:** This research was funded by the National Research, Development and Innovation Office (Budapest, Hungary), grant numbers TKP2020 IES, Grant No. BME-IE-BIO, and OTKA, SNN-125637 and PD-131467.

**Acknowledgments:** A.O.I. acknowledges Stipendium Hungaricum Scholarship Program for supporting the research work and his Ph.D. study.

**Conflicts of Interest:** The authors declare no conflict of interest. The funders had no role in the design of the study; in the collection, analyses, or interpretation of data; in the writing of the manuscript, or in the decision to publish the results.

## References

1. Poppe, L.; Vértessy, B.G. The Fourth Wave of Biocatalysis Emerges—The 13<sup>th</sup> International Symposium on Biocatalysis and Biotransformations. *ChemBioChem* **2018**, *19*, 284–287. [[CrossRef](#)]
2. Bornscheuer, U.T. The fourth wave of biocatalysis is approaching. *Philos. Trans. R. Soc. A Math. Phys. Eng. Sci.* **2018**, *376*, 20170063. [[CrossRef](#)]
3. Najafpour, G.D. Chapter 6—Bioreactor Design. In *Biochemical Engineering and Biotechnology*; Elsevier: Amsterdam, The Netherlands, 2007; pp. 142–169. ISBN 9780444528452.
4. Hershler, A. Fluid Treating Method and Apparatus. U.S. Patent 3,219,318A, 23 November 1965.
5. Hershler, A. Improvements in Fluid Treating Method and Apparatus. GB Patent 1,113,046A, 8 May 1968.
6. Barabash, V.M.; Abiev, R.S.; Kulov, N.N. Theory and Practice of Mixing: A Review. *Theor. Found. Chem. Eng.* **2018**, *52*, 473–487. [[CrossRef](#)]
7. Ou, Z.; Pan, J.; Tang, L.; Shi, H. Continuous enantiomer-selective acylation reaction of 1-phenylethanamine in a magnetic fluidized bed reactor system (MFBR). *J. Chem. Technol. Biotechnol.* **2019**, *94*, 1951–1957. [[CrossRef](#)]
8. Reichert, C.; Hoell, W.H.H.; Franzreb, M. Mass transfer enhancement in stirred suspensions of magnetic particles by the use of alternating magnetic fields. *Powder Technol.* **2004**, *145*, 131–138. [[CrossRef](#)]
9. Román-Pizarro, V.; Ramírez-Gutiérrez, M.; Gómez-Hens, A.; Fernández-Romero, J.M. Usefulness of magnetically-controlled MNPs-enzymes microreactors for the fluorimetric determination of total cholesterol in serum. *Talanta* **2020**, *208*, 120426. [[CrossRef](#)]
10. Furdui, V.I.; Harrison, D.J. Immunomagnetic T cell capture from blood for PCR analysis using microfluidic systems. *Lab. Chip.* **2004**, *4*, 614. [[CrossRef](#)] [[PubMed](#)]
11. Gebreyohannes, A.Y.; Giorno, L.; Vankelecom, I.F.J.; Verbiest, T.; Aimar, P. Effect of operational parameters on the performance of a magnetic responsive biocatalytic membrane reactor. *Chem. Eng. J.* **2017**, *308*, 853–862. [[CrossRef](#)]
12. Hajar, M.; Vahabzadeh, F. Biolubricant production from castor oil in a magnetically stabilized fluidized bed reactor using lipase immobilized on  $Fe_3O_4$  nanoparticles. *Ind. Crops Prod.* **2016**, *94*, 544–556. [[CrossRef](#)]

13. Zheng, D.; Wang, S.; Qiu, S.; Lin, J.; Diao, X. Synthesis of butyl oleate catalyzed by cross-linked enzyme aggregates with magnetic nanoparticles in rotating magneto-micro-reactor. *J. Biotechnol.* **2018**, *281*, 123–129. [[CrossRef](#)]
14. Croat, J.J.; Herbst, J.F.; Lee, R.W.; Pinkerton, F.E. Pr-Fe and Nd-Fe-based materials: A new class of high-performance permanent magnets. *J. Appl. Phys.* **1984**, *55*, 2078–2082. [[CrossRef](#)]
15. Sagawa, M.; Fujimura, S.; Togawa, N.; Yamamoto, H.; Matsuura, Y. New material for permanent magnets on a base of Nd and Fe. *J. Appl. Phys.* **1984**, *55*, 2083–2087. [[CrossRef](#)]
16. Li, F.; Wu, W.; Ning, A.; Wang, J. Surface Functionalization and Magnetic Motion of Hydrophobic Magnetic Nanoparticles with Different Sizes. *Int. J. Chem. React. Eng.* **2015**, *13*, 113–118. [[CrossRef](#)]
17. Pálovics, P.; Németh, M.; Rencz, M. Investigation and Modeling of the Magnetic Nanoparticle Aggregation with a Two-Phase CFD Model. *Energies* **2020**, *13*, 4871. [[CrossRef](#)]
18. Weiser, D.; Bencze, L.C.; Bánóczy, G.; Ender, F.; Kiss, R.; Kókai, E.; Szilágyi, A.; Vértessy, B.G.; Farkas, Ö.; Paizs, C.; et al. Phenylalanine Ammonia-Lyase-Catalyzed Deamination of an Acyclic Amino Acid: Enzyme Mechanistic Studies Aided by a Novel Microreactor Filled with Magnetic Nanoparticles. *ChemBioChem* **2015**, *16*, 2283–2288. [[CrossRef](#)] [[PubMed](#)]
19. Ender, F.; Weiser, D.; Nagy, B.; Bencze, C.L.; Paizs, C.; Pálovics, P.; Poppe, L. Microfluidic multiple cell chip reactor filled with enzyme-coated magnetic nanoparticles—An efficient and flexible novel tool for enzyme catalyzed biotransformations. *J. Flow Chem.* **2016**, *6*, 43–52. [[CrossRef](#)]
20. Wei, W.; Wang, Z. Investigation of Magnetic Nanoparticle Motion under a Gradient Magnetic Field by an Electromagnet. *J. Nanomater.* **2018**, *2018*, 6246917. [[CrossRef](#)]
21. Arsalan, A.; Younus, H. Enzymes and nanoparticles: Modulation of enzymatic activity via nanoparticles. *Int. J. Biol. Macromol.* **2018**, *118*, 1833–1847. [[CrossRef](#)] [[PubMed](#)]
22. Bilal, M.; Zhao, Y.; Rasheed, T.; Iqbal, H.M.N. Magnetic nanoparticles as versatile carriers for enzymes immobilization: A review. *Int. J. Biol. Macromol.* **2018**, *120*, 2530–2544. [[CrossRef](#)]
23. Viola, R.E. L-Aspartase: New Tricks from an Old Enzyme. In *Advances in Enzymology and Related Areas Molecular Biology*; John Wiley & Sons Inc.: New York, NY, USA, 2000; Volume 74, pp. 295–341. ISBN 0471349216.
24. Fibriansah, G.; Veetil, V.P.; Poelarends, G.J.; Thunnissen, A.-M.W.H. Structural Basis for the Catalytic Mechanism of Aspartate Ammonia Lyase. *Biochemistry* **2011**, *50*, 6053–6062. [[CrossRef](#)]
25. De Villiers, M.; Puthan Veetil, V.; Raj, H.; de Villiers, J.; Poelarends, G.J. Catalytic Mechanisms and Biocatalytic Applications of Aspartate and Methylaspartate Ammonia Lyases. *ACS Chem. Biol.* **2012**, *7*, 1618–1628. [[CrossRef](#)] [[PubMed](#)]
26. Asano, Y.; Kira, I.; Yokozeki, K. Alteration of substrate specificity of aspartase by directed evolution. *Biomol. Eng.* **2005**, *22*, 95–101. [[CrossRef](#)]
27. Van der Werf, M.J.; van den Tweel, W.J.J.; Kamphuis, J.; Hartmans, S.; de Bont, J.A.M. The potential of lyases for the industrial production of optically active compounds. *Trends Biotechnol.* **1994**, *12*, 95–103. [[CrossRef](#)]
28. Weiner, B.; Poelarends, G.J.; Janssen, D.B.; Feringa, B.L. Biocatalytic Enantioselective Synthesis of *N*-Substituted Aspartic Acids by Aspartate Ammonia Lyase. *Chem. A Eur. J.* **2008**, *14*, 10094–10100. [[CrossRef](#)]
29. Li, R.; Wijma, H.J.; Song, L.; Cui, Y.; Otzen, M.; Tian, Y.; Du, J.; Li, T.; Niu, D.; Chen, Y.; et al. Computational redesign of enzymes for regio- and enantioselective hydroamination. *Nat. Chem. Biol.* **2018**, *14*, 664–670. [[CrossRef](#)] [[PubMed](#)]
30. Csuka, P.; Molnár, Z.; Tóth, V.; Weiser, D.; Vértessy, B.G.; Poppe, L. Characterization of the Aspartate Ammonia-lyase from *Pseudomonas fluorescens* R124-Kinetics and Immobilization on Magnetic Nanoparticles. *ChemBioChem* **2021**, submitted.
31. Engasser, J.-M.; Horvath, C. Diffusion and Kinetics with Immobilized Enzymes. In *Immobilized Enzyme Principles*; Academic Press, Inc.: Cambridge, MA, USA, 1976; Volume 1, pp. 127–220.
32. Cimetta, E.; Figallo, E.; Cannizzaro, C.; Elvassore, N.; Vunjak-Novakovic, G. Micro-bioreactor arrays for controlling cellular environments: Design principles for human embryonic stem cell applications. *Methods* **2009**, *47*, 81–89. [[CrossRef](#)] [[PubMed](#)]
33. Darwesh, O.M.; Ali, S.S.; Matter, I.A.; Elsamahy, T.; Mahmoud, Y.A. Enzymes immobilization onto magnetic nanoparticles to improve industrial and environmental applications. In *Methods in Enzymology*; Elsevier Inc.: Amsterdam, The Netherlands, 2020; Volume 630, pp. 481–502. ISBN 9780128201435.
34. Yadav, N.; Narang, J.; Chhillar, A.K.; Pundir, C.S. Preparation, Characterization, and Application of Enzyme Nanoparticles. In *Methods in Enzymology*; Elsevier Inc.: Amsterdam, The Netherlands, 2018; Volume 609, pp. 171–196. ISBN 9780128152409.